Journal of Magnetism and Magnetic Materials 321 (2009) 3933–3937

Contents lists available at ScienceDirect

Journal of Magnetism and Magnetic Materials

journal homepage: www.elsevier.com/locate/jmmm

The effect of Gd-doping on the charge ordering state of $Bi_{0.3-x}Gd_xCa_{0.7}MnO_3$ ($0 \le x \le 0.30$)

R.R. Zhang [a], G.L. Kuang [a,*], X. Luo [b], Y.P. Sun [b]

[a] High Magnetic Field Laboratory, Chinese Academy of Sciences, Hefei 230031, People's Republic of China
[b] Key Laboratory of Materials Physics, Institute of Solid State Physics, Chinese Academy of Sciences, Hefei 230031, People's Republic of China

ARTICLE INFO

Article history:
Received 15 September 2008
Received in revised form
8 July 2009
Available online 3 August 2009

PACS:
71.27.+a
71.30.+h
75.47.Lx

Keywords:
Charge ordering
Magnetic transition
Manganite

ABSTRACT

The effect of Gd-doping on the charge ordering (CO) state in perovskite-type manganates $Bi_{0.3-x}Gd_xCa_{0.7}MnO_3$ with $x = 0$, 0.02, 0.05, 0.1, 0.3 has been investigated by transport and magnetic property measurements. It is found that CO temperature (T_{CO}) and antiferromagnetic (AFM) ordering temperature T_N occurring below T_{CO} decrease obviously with increasing Gd-doping level. Accompanying the variation of T_{CO}, the increased magnetization and the decreased resistivity are observed. In addition, the increased magnetic inhomogeneity has been also observed in the samples based on the difference between the zero-field-cooling (ZFC) magnetization M_{ZFC} and field-cooling (FC) magnetization M_{FC}, which is ascribed to the competition between ferromagnetic (FM) phase induced by Gd-doping and CO AFM phase. The experimental results indicate that the Bi^{3+} lone pair electron with $6s^2$ character plays a dominating role on the CO state of $Bi_{0.3}Ca_{0.7}MnO_3$.

1. Introduction

Manganese oxides with perovskite structure have been the subject of vivid interest in recent years because of their exotic electronic and magnetic properties [1–3]. These manganites present a colossal magnetoresistance (CMR) effect and many theories have been proposed to explain the mechanism about CMR such as double exchange (DE) [4], polaronic effects [5] and phase separation combined with percolation [6]. Besides CMR effect, CO phenomenon [7,8] present in those compounds has also attracted a lot of attention. CO in the manganites is generally characterized by the direct space ordering of Mn^{3+} and Mn^{4+} ions [8]. Many studies show that CO state and concomitant spin and/or orbital ordering (OO) are favored when the long-range coulomb interaction and/or a strong electron–lattice interaction due to Jahn–Teller (JT) distortion overcome the kinetic energy of e_g electrons [9–11].

The one electron bandwidth tuning mechanism has been widely used to quantitatively justify T_{CO} variation in the $Ln_{1-x}A_xMnO_3$ family of compounds [12,13]. Wide e_g bandwidths, i.e., large mean size of the A-site cations $\langle r_A \rangle$, favor the mobility of the itinerant electrons through the lattice which results in the decrease of T_{CO}, while narrow bandwidths induce an opposite variety. For bismuth based manganites, there is a Bi^{3+} lone pair with $6s^2$ character in them, which is proposed to justify the strong tendency of the charges to localize and order, so bismuth based manganites may do not follow the dependency of T_{CO} on $\langle r_A \rangle$ mechanism as the lanthanide ones. An orientation of the $6s^2$ lone pair toward a surrounding anion (O 2p) can produce a local distortion or even hybridization between Bi-6s-orbits and O-2p-orbits [14]. As a result, the movement of e_g electrons through the Mn–O–Mn bridges can be severely reduced and the charge order tendency is strongly favored. As we known, although several works have reported the Bi doped effect on different manganite samples [15–18], the physical feather of CO is still unclear. Additionally, previous studies focused on the large ion size of lanthanides and many of the end compounds were hole doped samples with FM state, while the electron doped ones were rarely studied. To understand the influence of the $\langle r_A \rangle$ and the Bi^{3+} lone pair with $6s^2$ on T_{CO} of $Bi_{0.3}Ca_{0.7}MnO_3$, we have substituted Gd^{3+} ions for Bi^{3+} ions because the Gd^{3+} ion has smaller ion size than the Bi^{3+} ion and the quenching of orbital angular momentum. In this paper, we have systemically studied the influence of the Gd-doping on the structural, magnetic and electronic transport properties of $Bi_{0.3-x}Gd_xCa_{0.7}MnO_3$ ($x = 0$, 0.02, 0.05, 0.1 and 0.3) (BGCMO) and found that T_{CO} decreases with increasing Gd content.

2. Experimental

Samples with composition $Bi_{0.3-x}Gd_xCa_{0.7}MnO_3$ ($x = 0$, 0.02, 0.05, 0.1 and 0.3) were synthesized by a common solid state

* Corresponding author. Tel.: +86 551 559 2002; fax: +86 551 559 1149.
E-mail address: kuang_gl@ipp.ac.cn (G.L. Kuang).

0304-8853/$ - see front matter © 2009 Elsevier B.V. All rights reserved.
doi:10.1016/j.jmmm.2009.07.054

reaction. A stoichiometric mixture of Bi_2O_3, Gd_2O_3, $CaCO_3$ and MnO_2 was ground and pressed into pellets, which were heated in air at 1023 and 1223 K for 20 h with intermediate grinding. Then the homogenized powders were pressed into cylindrical pellets, and were subjected to heat treatment for 20 h at 1273 K. After calcinations, the samples were reground, pelletized again, and the final heat treatment was performed for 20 h at 1373 K in air for $x \leq 0.1$, at 1473 K for $x = 0.3$.

Powder X-ray diffraction measurement was performed using a Philips X'pert PRO X-ray diffractmeter with Cu K_α radiation at room temperature. The temperature dependence of magnetization was measured using a quantum design superconducting quantum interference device (SQUID) MPMS system (5 K $\leq T \leq$ 400 K, 0 A/m $\leq H \leq$ 3979 kA/m). The resistivity ρ was measured by means of a quantum design physical properties measurements system (PPMS) (5 K $\leq T \leq$ 400 K, 0 A/m $\leq H \leq$ 7162 k kA/m) using the standard four-probe method.

3. Results and discussion

The room temperature XRD patterns of BGCMO are shown in Fig. 1. It indicates that all the samples are single phase with no detectable secondary phases. All diffraction peaks can be indexed by orthorhombic lattice with the space group *Pnma*. The lattice parameters can be obtained by fitting the experimental spectra using the standard Rietveld technique [19]. The results are shown in Fig. 2. Clearly, with the increasing of Gd content, the unit-cell volume decreases monotonously, this is consistent with the fact that the Gd^{3+} ion (1.053 Å) has a smaller ionic radius than that of the Bi^{3+} ion (1.17 Å). Additionally, the cell parameters of the samples obey the relation $b/\sqrt{2} < c < a$ (shown in the inset of Fig. 2). The combination of octahedral tilting and a cooperative JT distortion is known to produce such O'-type distorted perovskite structures [20].

The temperature dependence of the dc magnetization $M(T)$ measured in the zero-field-cooled (M_{ZFC}) and field-cooled (M_{FC}) modes at a magnetic field of 7958 A/m for all the samples is shown in Fig. 3. At high temperature, all of the samples are in the paramagnetic (PM) state. In order to study the magnetic interaction in PM region, $M(T)$ data have been fitted according to the Curie–Weiss law, $\chi = C/(T-\theta_P)$, as shown in Fig. 4. The effect magnetic moment μ_{eff} can be obtained as 5.88, 5.09, 5.16, 6.06, 6.64 and 6.65μ_B for the samples with $x = 0$, 0.02, 0.05, 0.1, 0.2 and 0.3, respectively and the PM Curie temperature θ_P are 95, 118, 123, 80 and 82 K. Subtracting the contribution of the Gd ions, the effect magnetic moment μ_{eff} for Mn ions are 5.88, 4.96, 4.84, 5.52, 5.61 and 5.03μ_B for the samples with $x = 0$, 0.02, 0.05, 0.1, 0.2 and 0.3, respectively. According to mean field approximation, the expected effective magnetic moment μ_{eff} can be calculated as 4.18μ_B, which is smaller than the values of the experiment, implying that the possible appearance of magnetic clusters in PM region due to the short range FM interaction [21]. With the decrease of temperature, the $M(T)$ curves of all the samples exhibit distinct maximum at certain temperatures (T_{CO}). According to the studies of neutron diffraction reported in previous literatures [22,23], these maximum can be attributed to the CO-paramagnetic (PM) transition. For the $x = 0$ sample, $T_{CO} = 287$ K, is similar to the result reported by Bokov et al. [24]. With the increasing of the Gd-doped level, T_{CO} decreases from 287 K for $x = 0$ to 237 K for $x = 0.3$, as shown in Fig. 5. It is well-known that the long-range coulomb interaction and the strong electron–lattice coupling induced by JT distortion favor the CO state in manganites. Therefore, the decreasing of T_{CO} may be induced by many factors, such as JT Mn^{3+} ion and the character of A-site ions. In our case, the carrier concentration (Mn^{3+}/Mn^{4+} ratio) keeps to be fixed by the equivalent substitution Gd^{3+} ions for Bi^{3+} ions, so the above phenomena may be induced by the characteristic difference

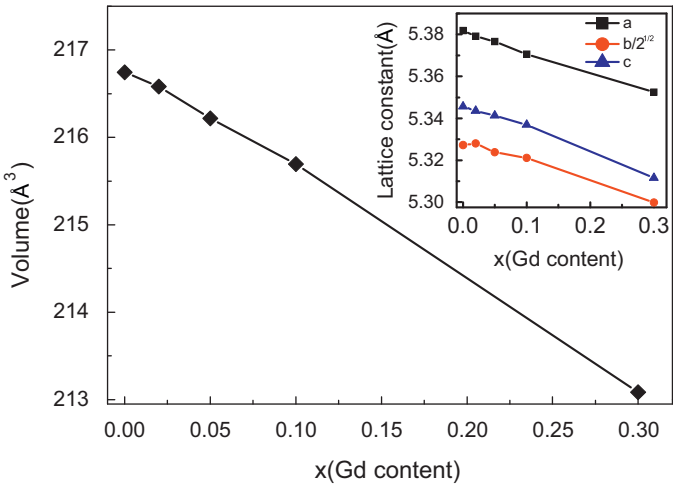

Fig. 2. Gd-doping level dependence of the unit cell volume *V*. The inset shows the lattice parameters *a*, $b/\sqrt{2}$and *c*.

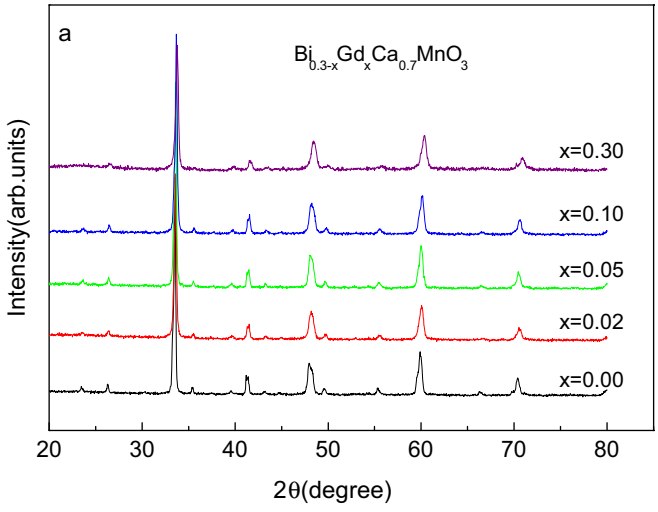

Fig. 1. X-ray diffraction patterns for BGCMO samples at room temperature.

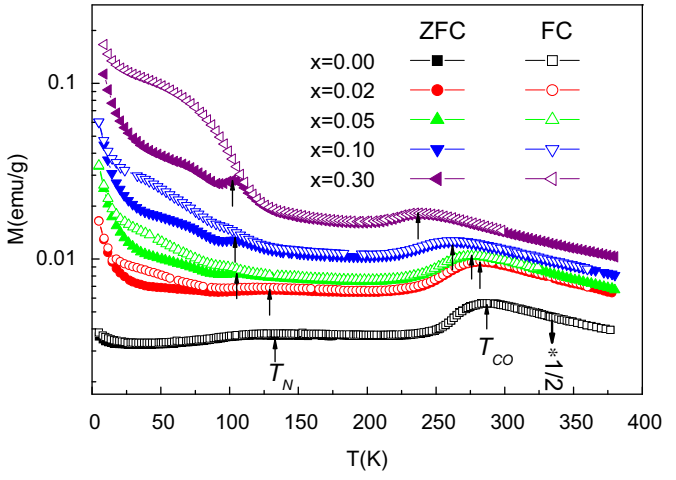

Fig. 3. Magnetization as a function of temperature $M(T)$ for BGCMO measured under $H = 7958$ A/m.

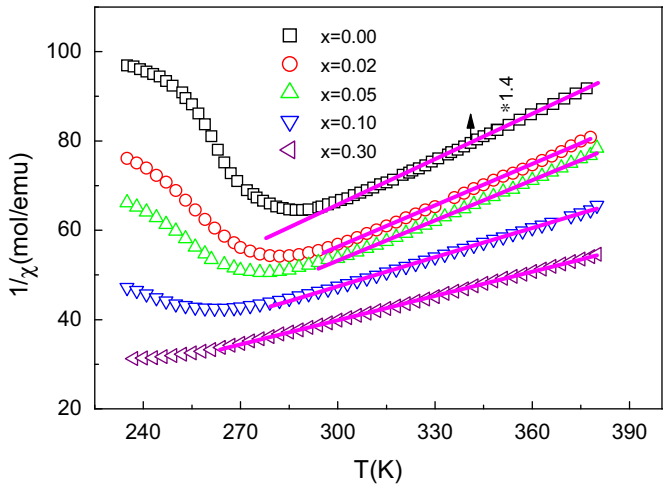

Fig. 4. The temperature dependence of the inverse of the magnetic susceptibility for BGCMO samples. The lines are the calculated curves according to the Curie–Weiss law.

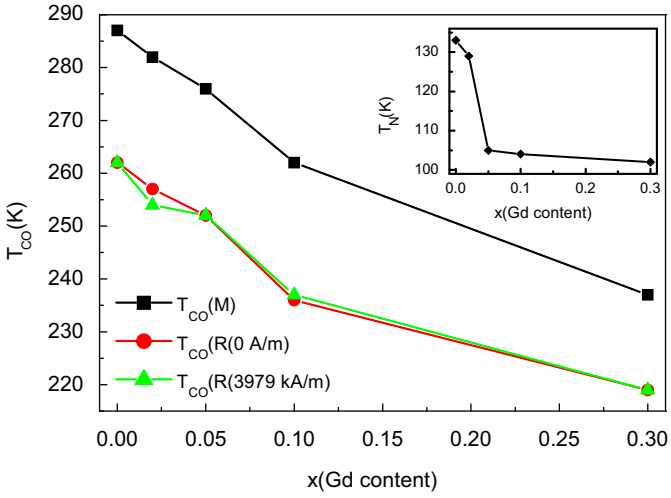

Fig. 5. The charge-ordering temperature (T_{CO}) variation versus x in the BGCMO system. $T_{CO}(M)$ is the CO temperature defined from $M(T)$ curves. $T_{CO}(R(0\,\text{A/m}))$ and $T_{CO}(R(3979\,\text{kA/m}))$ are the CO temperature defined from $\rho(T)$ curves measured at 0 and 3979 kA/m, respectively. The inset shows the antiferromagnetic order temperature T_N variation versus x.

between Gd^{3+} and Bi^{3+} ions. First, Gd^{3+} and Bi^{3+} ions have different ion sizes, where the effective ion size of Gd^{3+} ($r_i = 1.053$ Å) is smaller than that of Bi^{3+} ($r_i = 1.17$ and 1.24 Å when lone pair character is constrained or dominant respectively) [25]. Thus, with the increasing of the Gd^{3+} content, the $\langle r_A \rangle$ decreases. Previous literatures proved that T_{CO} increased with the decreasing of the $\langle r_A \rangle$ [12,26–28]. That is to say, the change of the $\langle r_A \rangle$ cannot be considered as the reason giving rise in the decrease of T_{CO} observed in our studied samples. Secondly, the Gd^{3+} ion with a half-filled 4f shell is a magnetic ion while the Bi^{3+} ion is not. In order to investigate the Gd ions' magnetic effect on the T_{CO}, the PM M–T curves of Gd^{3+} have been calculated by Brillouin function:

$$\mu = Jg_J\mu_B B_J(x),$$

where $B_J(x) = (1+1/2J)\coth[(1+1/2J)x] - (1/2J)\coth(x/2J)$ and $x = Jg_J\mu_B B/k_B T$ neglecting the weak crystal field effect as shown by circle symbol in Fig. 6. To take $x = 0.1$ sample as an example, through subtracting the PM moment of Gd^{3+} ions from the M–T curve, we can obtain M–T curve as shown by trigonal symbol in Fig. 6. The result displays that the T_{CO} does not change, meaning

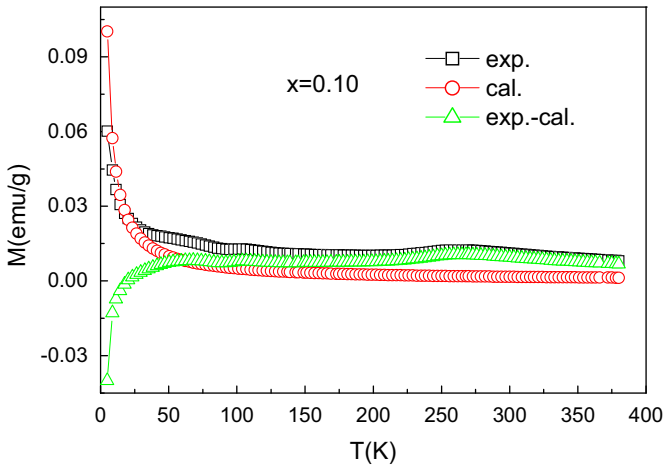

Fig. 6. Temperature dependence of the magnetization of $x = 0.10$ sample (hollow square symbol) measured under a field of 7958 A/m from 5 to 380 K by warming process in zero-field-cooled mode and Gd^{3+} (hollow circle symbol) calculated by Brillouin function. The M–T curve after subtracting moment of Gd ions is present by hollow trigonal symbol.

that the magnetism of Gd^{3+} ions has no effect on CO behavior in the studied manganites. This result is reasonable since the magnetic interactions of the 4f ions are much weaker (the ordering temperature is usually <10 K) than those of Mn ions. Moreover, the value of M–T curve with subtracting moment of Gd ions is negative at low temperatures, indicating that Gd^{3+} ions are not completely PM at low temperatures. The similar results were also reported in other systems in previous literatures [28–31]. Thirdly, Bi^{3+} ion has a lone pair with strong $6s^2$ character. Theoretical calculation has showed that off-center shifts of the ions with ns^2 electronic configuration (hence, the structural distortion in a crystal) can take place to reach an energy reduction [32]. Many previous experiments proved that bismuth based manganites such as $Bi_{1-x}Sr_xMnO_3$ have high T_{CO} related to this $6s^2$ lone pair which can induce a large distortion in the structure. Therefore, the decrease of T_{CO} may be attributed to the weakening of the distortion due to the reduction of $6s^2$ lone pair because of the Gd ions substitution for Bi ions. Additionally, it is found that the magnetization increases with the increasing of Gd-doping level in the measured temperature range as shown in Fig. 3, which is also suggested to originate from the same reason.

As it is well-known, for manganites, the appearance of CO state usually accompanies the occurring of AFM interaction. For all of the samples, below T_{CO}, AFM superexchange interaction dominates [24], leading to an AFM ordering at a temperature T_N. Fig. 3 shows that T_N also decreases with increasing Gd-doping level, which is similar to the behavior of T_{CO}. The monotonous reduction behavior of T_{CO} and T_N with increasing Gd-doping content is plotted in main panel and inset of Fig. 5. Moreover, it is found that the M_{ZFC} curves of all of the samples begin to deviate from the M_{FC} ones below T_N and the difference become larger with the increasing of Gd content as shown in Fig. 3. Similar phenomena were also reported in other manganites [33,34], which were suggested to stem from the existence of small magnetic clusters and magnetic anisotropy, respectively. For our samples, the difference between M_{ZFC} and M_{FC} curves is suggested to originate from the magnetic inhomogeneity due to the competition between DE FM and CO AFM interactions. As described above, the increasing amount of Gd^{3+} ions, i.e., the decreasing of Bi^{3+} ions, the distortion related to $6s^2$ lone pair of Bi^{3+} ions is weakened, which results in the enhancement of itinerant ability of e_g electrons and DE FM between Mn^{3+} and Mn^{4+}. In addition, from

Fig. 3, it is found that all M–T curves of the samples except for the $x = 0$ one display a distinct upturn behavior at low temperature, and the upturn temperature range increases with increasing x, which is suggested to be related to the increased PM moment of Gd ions.

To investigate the effect of Gd-doping on the magnetic properties further, the magnetization hysteresis loops of all the samples measured at the temperature of 5 K are shown in Fig. 7. It shows that the $x = 0$ sample has an almost linearly field-dependent magnetization, implying that the AFM property of no Gd-doping sample at low temperatures. However, for Gd-doping samples, the $M(H)$ curves behave as an obvious nonlinear behavior and tend to be saturated under high field. In order to find out the origin of this abnormal behavior, we fitted the experimental data of the $x = 0.3$ samples according to Langevin theory. In Langevin theory

$$M = N\mu L(\alpha),$$
$$L(\alpha) = \coth\alpha - 1/\alpha, \alpha = \mu B/k_B T.$$

The fitting parameters are the number N and average effective moment μ of magnetic ions in the manganite per gram. The fitted result is consistent with the experimental result quite well as shown in the inset of Fig. 7. This indicates that the magnetization at 5 K mainly comes from the PM contribution of the system. The fitting parameters N and μ are 0.0032 mol and $4.2\mu_B$ respectively. It is noticed that there are only 0.0022 mol Gd^{3+} ions in the $Gd_{0.3}Ca_{0.7}MnO_3$ manganite per gram, which is smaller than the fitting parameter. This fact means that the PM behavior of both Mn^{3+} and Mn^{4+} ions makes the contribution to magnetization as well, and $\mu = 4.2\mu_B$ is the average effective moment for Mn^{3+}, Mn^{4+}, and Gd^{3+} ions. It is well-known that only when $\alpha \ll 1$ Langevin function $L(\alpha) = \mu H/3kT$, and the M–H curve behaves as a straight line. This is just the reason why M–H curve at 5 K deviates from a straight line. Based on the above experimental results, it can be concluded that the magnetization in M–T curve at low temperatures originates from the PM contribution of magnetic ions. Similar result was also reported by Ling et al. [35].

To investigate the effect of Gd-doping on the transport properties of the samples. The temperature dependence of resistivity $\rho(T)$ of the samples has been measured in the temperature range from 5 to 380 K at zero field. The measuring results are plotted in Fig. 8. It shows that all samples exhibit insulating behaviors over whole measuring temperature range and the resistivity decreases with the increasing of Gd-doping content blow the temperature of T_{CO}. Using $d(\ln\rho)/d(1/k_BT)$ as a function of temperature [36], we can define the T_{CO} (the peak of the curve, not shown here), which decreases with the increasing of Gd-doping content(as shown in Fig. 4). The resistivity of all samples at 3979 kA/m has been also measured and T_{CO} almost does not change for the applied and without magnetic fields, which indicates that magnetic field does not change T_{CO}. The resistivity can be best fitted with the small polaron hopping conduction (SPC) model $\rho \sim T\exp(E_a/T)$ and the Mott's variable range hopping (VRH) model $\rho \sim \exp(T_0/T)^{1/4}$ in the high measuring temperature range and low temperature range, respectively, consistent with the reported results in the literatures [37,38]. The fitting results are shown in the inset of Fig. 8 and the fitted parameters are summarized in Table 1. The results show that T_0 decreases with the increasing of Gd-doping level, and T_0 is related to the localization length ξ by the relation $k_BT_0 = 24/(\pi N(E_F)\xi^3)$ [39], provided $N(E_F)$ does not change, meaning that the localization length ξ increases with the Gd-doping content. This is to say, the carriers become less localized with the increasing of Gd-doping content. For our samples, the substitution of Gd^{3+} ions with a smaller ion size for Bi^{3+} ions not only reduces the $\langle r_A \rangle$, but also induces disorder of A site, which is expected to cause the increase of the resistivity of the samples. However, the observed results are opposite to the expected ones. The origin of this phenomenon is also suggested to ascribe to the weakening of the distortion due to the reduction of $6s^2$ lone pair because of the Gd ions substitution for Bi ions as mentioned above. The conclusion obtained from the electronic transport is consistent with that from the magnetization. That is to say, for Bi-based manganites with CO state, the Bi^{3+} lone pair electron with $6s^2$ character plays a dominating role on the electronic and magnetic properties.

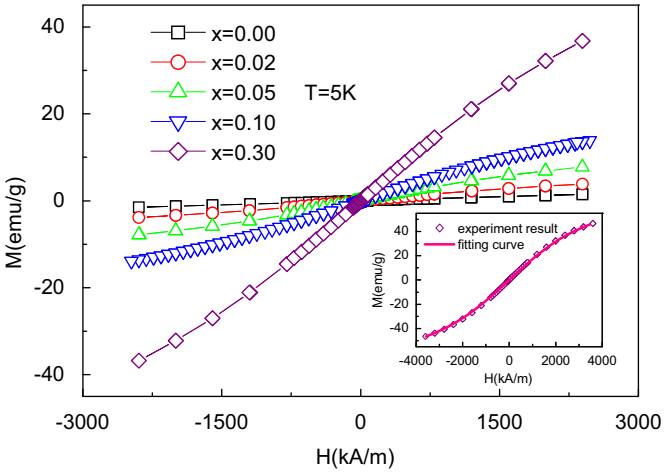

Fig. 7. Field dependence of the magnetization $M(H)$ for BGCMO measured at $T = 5$ K. The inset shows the $x = 0.30$ sample measured under applied magnetic field up to 3581 kA/m and the fitting of magnetic field dependence of magnetization at 5 K by Langevin theory.

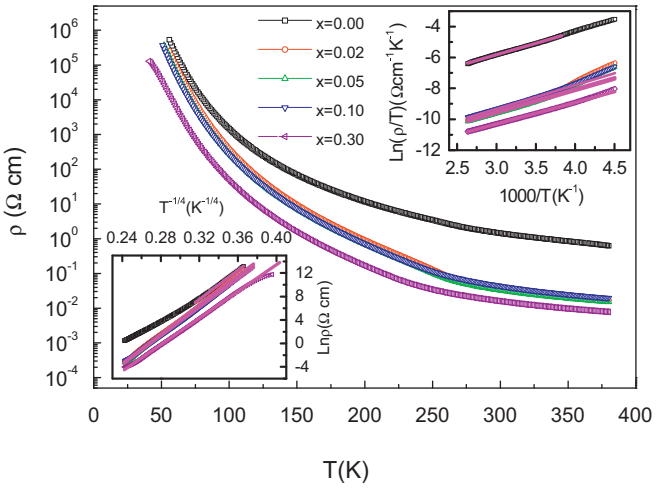

Fig. 8. The temperature dependence of resistivity $\rho(T)$ for BGCMO samples and the up-right inset and down-left inset display the fitting curves of $\rho(T)$ by SPC and VRH, respectively.

Table 1
Parameters of the studied samples in this work.

x	0	0.02	0.05	0.10	0.30
E_a (eV)	0.127	0.127	0.122	0.132	0.120
T_0 (10^8 K)	2.408	2.407	2.331	2.137	1.688

x stands for the Gd-doping level (x). E_a is the fitting parameter of $\rho(T)$ curves according to the SPC model. T_0 is the fitting parameter of $\rho(T)$ curves according to the VRH model (see text).

4. Conclusions

In summary, structural, magnetic and electronic properties of BGCMO samples with CO state have been studied systematically. With increasing Gd-doping level T_{CO} decreases and it is independent of the moments of the Gd^{3+} ions. Accompanying the variation of T_{CO}, the increased magnetization and the decreased resistivity are observed. Considering the effective ion size of Gd^{3+} is smaller than that of Bi^{3+} and the lone pair with strong $6s^2$ character of Bi^{3+} ions, the decreasing of T_{CO} and complex magnetic properties result mainly from the effect of the $6s^2$ lone pair of Bi^{3+} ion on the e_g electrons transport from Mn^{3+} to Mn^{4+} through the O 2p in Mn–O–Mn bonds. In a word, the experimental results show that although the $6s^2$ lone pair of Bi^{3+} is strongly screened in the calcium doped bismuth based manganites, it plays an important role in the CO state of $Bi_{0.3}Ca_{0.7}MnO_3$.

Acknowledgments

This work was supported by the National Key Basic Research under Contract no. 2007CB925002, and the National Nature Science Foundation of China under Contract nos. 10774146, 50672099 and Director's Fund of Hefei Institutes of Physical Science, Chinese Academy of Sciences.

References

[1] S. Jin, T.H. Tiefel, M. McCormack, R.A. Fastnacht, R. Ramesh, L.H. Chen, Science 264 (1994) 413.
[2] Y. Tokura, Y. Tomioka, H. Kuwahara, A. Asamitsu, Y. Moritomo, M. Kasai, J. Appl. Phys. 79 (1996) 5288.
[3] J.M.D. Coey, M. Viret, S. Von Molnar, Adv. Phys. 48 (1999) 167.
[4] C. Zener, Phys. Rev. 82 (1951) 403.
[5] A.J. Millis, P.B. Littlewood, B.I. Shraiman, Phys. Rev. Lett. 74 (1995) 5144.
[6] S. Mori, C.H. Chen, S.W. Cheong, Phys. Rev. Lett. 81 (1998) 3972.
[7] J.B. Goodenough, Phys. Rev. 100 (1955) 564.
[8] P.G. Radaelli, D.E. Cox, M. Marezio, S.W. Cheong, Phys. Rev. B 55 (1997) 3015.
[9] P.G. Radaelli, D.E. Cox, L. Capogna, S.W. Cheong, M. Marezio, Phys. Rev. B 59 (1999) 14440.
[10] S. Yunoki, T. Hotta, Phys. Rev. Lett. 84 (2000) 3714.
[11] Y. Tokura, N. Nagaosa, Science 288 (2000) 21.
[12] C.N.R. Rao, A. Arulraj, P.N. Santosh, A.K. Cheetham, Chem. Mater. 10 (1998) 2714.
[13] J. Fontcuberta, B. Martínez, A. Seffar, S. Piñol, J.L. García-Muñoz, X. Obradors, Phys. Rev. Lett. 76 (1996) 1122.
[14] N.A. Hill, K.M. Rabe, Phys. Rev. B 59 (1999) 8759.
[15] J.R. Sun, J. Gao, Y. Fei, R.W. Li, B.G. Shen, Phys. Rev. B 67 (2003) 144414.
[16] L. Righi, J. Gutiérrez, J.M. Barandiarán, J. Phys.: Condens. Matter 11 (1999) 2831.
[17] I. Kammoun, W. Cheikhrouhou-Koubaa, W. Boujelben, A. Cheikhrouhou, J. Mater. Sci. 43 (2008) 960.
[18] S. Savitha Pillai, P.N. Santhosh, N. Harish Kumar, P. John Thomas, F. Tuna, J. Phys.: Condens. Matter 21 (2009) 195409.
[19] D.B. Wiles, R.A. Young, J. Appl. Cryst. 14 (1981) 149.
[20] J.B. Goodenough, A. Wold, R.J. Arnott, N. Menyuk, Phys. Rev. 124 (1961) 373.
[21] J.M. De Teresa, M.R. Ibarra, P.A. Algarabel, C. Ritter, C. Marquina, J. Blasco, J. Garcia, A. del Moral, Z. Arnold, Nature 386 (1997) 256.
[22] E.I. Turkevich, V.P. Plakhitii, Fiz. Tverd. Tela (Leningrad) 10 (1968) 951.
[23] W. Bao, J.D. Axe, C.H. Chen, S.W. Cheong, Phys. Rev. Lett. 78 (1997) 543.
[24] V.A. Bokov, N.A. Grigoryan, M.F. Bryzhina, Phys. Status Solidi 20 (1967) 745.
[25] R.D. Shannon, Acta Cryst. A 32 (1976) 751.
[26] P.M. Woodward, T. Vogt, D.E. Cox, A. Arulraj, C.N.R. Rao, P. Karen, A.K. Cheetham, Chem. Mater. 10 (1998) 3652.
[27] A. Arulraj, P.N. Santosh, R.S. Gopalan, A. Guha, A.K. Raychaudhuri, N. Kumar, C.N.R. Rao, J. Phys.: Condens. Matter 10 (1998) 8497.
[28] L.S. Ling, J.Y. Fan, L. Pi, Y. Ying, S. Tan, Y.H. Zhang, J. Phys.: Condens. Matter 20 (2008) 125214.
[29] R.W. Li, J.R. Sun, Q.A. Li, S.Y. Zhang, B.G. Shen, J. Magn. Magn. Mater. 265 (2003) 248.
[30] G.J. Snyder, C.H. Booth, F. Bridges, R. Hiskes, S. DiCarolis, M.R. Beasley, T.H. Geballe, Phys. Rev. B 55 (1997) 6453.
[31] O. Peña, M. Bahout, D. Gutierrez, P. Duran, C. Moure, Solid State Sci. 5 (2003) 1217.
[32] F. Sugawara, S. Iida, Y. Syono, S. Akimoto, J. Phys. Soc. Jpn. 25 (1968) 1553; F. Sugawara, S. Iida, Y. Syono, S. Akimoto, J. Phys. Soc. Jpn. 20 (1965) 1529.
[33] Darshan C. Kundaliya, Reeta Vij, R.G. Kulkarni, A.A. Tulapurkar, R. Pinto, S.K. Malik, W.B. Yelon, J. Magn. Magn. Mater. 264 (2003) 62.
[34] D. Tzankov, D. Kovacheva, K. Krezhov, R. Puźniak, A. Wiśniewski, E. Sváb, M. Mikhov, J. Phys.: Condens. Matter 17 (2005) 4319.
[35] L.S. Ling, J.Y. Fan, L. Pi, Y. Ying, S. Tan, Y.H. Zhang, Solid State Commun. 144 (2007) 189.
[36] K. Vijaya Sarathy, S. Parashar, A.R. Raju, C.N.R. Rao, Solid State Sci. 4 (2002) 353.
[37] C.M. Xiong, J.R. Sun, R.W. Li, S.Y. Zhang, T.Y. Zhao, B.G. Shen, J. Appl. Phys. 95 (2004) 1336.
[38] Sudipta Pal, Aritra Banerjee, P. Chatterjee, B.K. Chaudhuri, Phys. Status Solidi (b) 237 (2003) 513.
[39] N.F. Mott, E.A. Davis, Electronic Processes in Non-Crystalline Materials, Clarendon, Oxford, 1971.